JOURNAL OF GEOPHYSICAL RESEARCH, VOL. 106, NO. D24, PAGES 33,789–33,797, DECEMBER 27, 2001

Internal layer tracing and age-depth-accumulation relationships for the northern Greenland ice sheet

M. Fahnestock

Earth System Science Interdisciplinary Center, University of Maryland, College Park, Maryland

W. Abdalati[1] and S. Luo[2]

NASA Goddard Space Flight Center, Greenbelt, Maryland

S. Gogineni

Radar Systems and Remote Sensing Laboratory, University of Kansas, Lawrence, Kansas

Abstract. Clues to previous ice sheet structure and long-term glaciological processes are preserved in the internal layering configuration of the Greenland ice sheet. Information about these internal layers has been retrieved over many parts of the ice sheet with the University of Kansas ice-penetrating radar. We report on the coherence of these layers over very large distances, describe a method of tracing these layers along thousands of kilometers of flight line, and do so for one flight during the 1999 Program for Arctic Regional Climate Assessment (PARCA) aircraft campaign. We determine the ages of these layers, based on information at the GRIP ice core site, and extend these ages along the flight line to Camp Century, where they are compared to modeled-derived age estimates. These ages agree with each other to between 2 and 15%, differences that can be substantially reduced with minor changes to the model parameters (accumulation rate and shear layer depth). Finally, we are able to derive estimates of accumulation rates along the flight line by fitting the age-depth data from layer tracing to a Dansgaard-Johnsen model with a minimization technique, providing estimates that match recent accumulation patterns within a few centimeters per year.

1. Introduction

A record of past climates of the last tens of thousands of years is preserved in the Greenland ice sheet, both chemically and physically: chemically, in the isotope and particle data [e.g., *Dansgaard et al.*, 1973; *Hammer et al.*, 1978], and physically, in the layering structure of the ice [e.g., *Alley et al.*, 1993]. Numerous efforts have yielded great success in extracting the depth versus age relationship from analysis of isotopes such as oxygen 18 and deuterium [e.g., *Meese et al.*, 1994], from visual observation of strata produced from summertime insolation [e.g., *Alley et al.*, 1993], and from modeling [e.g., *Dansgaard and Johnson*, 1969]. However, the age-depth relationship has only been known at the locations of ice cores, and to date, means of spatially extending these records beyond those points, or linking layers of the ice in one location to those in another, have been limited to model-based estimates with little data for verification.

Ice-penetrating radar (IPR) has been flown over much of the Greenland [*Gudmandsen*, 1969; *Gogineni et al.*, this issue; *Bamber et al.*, this issue] and Antarctic [*Drewry*, 1983] ice sheets and used from the ground for local studies. It has long been realized as an effective technique for determining ice thickness and the depth distribution of "internal layers," which are thought to be isochronous surfaces [*Gudmandsen*, 1975; *Jacobel and Hodge*, 1995]. While the internal layering is in some areas, as measured by a number of instruments, discontinuous, it is relatively coherent when viewed over hundreds of kilometers. This maintenance of pattern, seen in Antarctica by *Drewry* [1983], is common among the records taken by the University of Kansas IPR [*Gogineni et al.*, 1998].

The large number of flight tracks (nearly 100,000 linear kilometers) collected in Greenland (Figure 1) with the University of Kansas IPR has made it worthwhile to develop a system for operator-assisted layer tracing, as it is possible to determine the layer configuration of the internal layers over much of the ice sheet. Using a system that we have developed around simple cross-correlation and peak-following techniques, we trace internal layers along a flight line through the GRIP site in central Greenland and across the ice sheet (Figure 2). The isochronous nature of layers and the dating provided by the GRIP core site allow us to determine the age-depth relationship in areas far removed from the ice core site and to demonstrate the potential for tying together core sites separated by large distances. Additionally, based on the age-

[1]Now at NASA Headquarters, Washington D. C.
[2]Employed by NVI Incorporated.

Copyright 2001 by the American Geophysical Union.

Paper number 2001JD900200.
0148-0227/01/2001JD900200$09.00

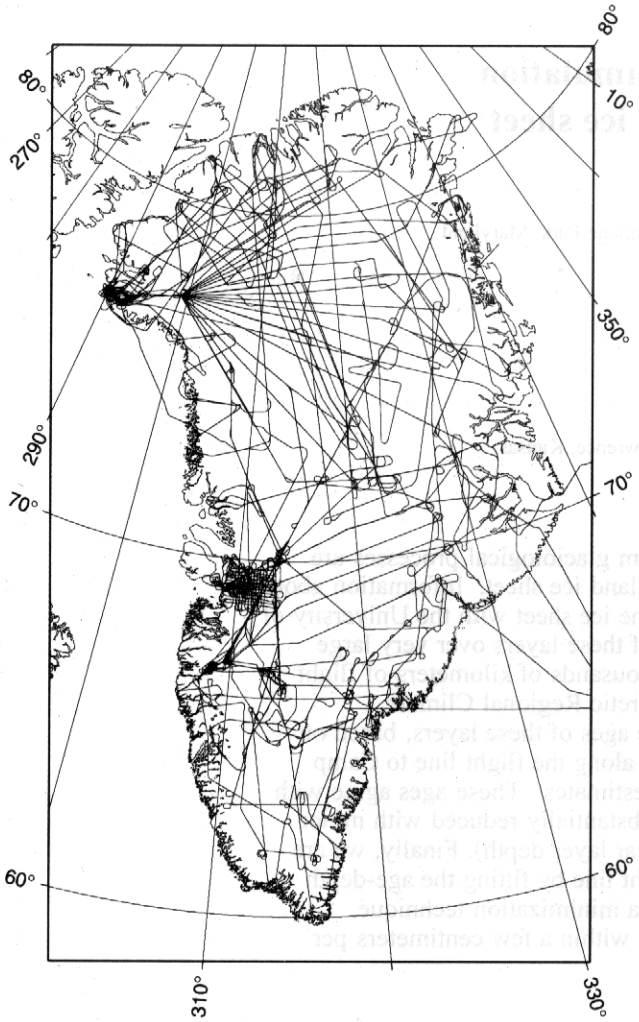

Figure 1. Aircraft flight lines on the Greenland ice sheet along which measurements were made with the University of Kansas ice penetrating radar (IPR).

depth relationships of these layers, we provide estimates of 10,000 year accumulation rates over a segment of the Greenland ice sheet. Knowledge of the age-depth relationship over large areas can be used to constrain flow models, providing insight not only into accumulation history but also to dynamics of ice flow.

2. Data Set

The instrument used to acquire the data was a pulse-compression coherent radar mounted on a NASA P-3 aircraft and is described in detail by *Gogineni et al.* [1998]. With a center frequency of 150 MHz and a 17 MHz bandwidth, the radar is capable of full penetration to the bedrock over most of the ice sheet area. The instrument generates a 1.6 μs pulse using a surface acoustic wave (SAW) expander. The signal peak power is 200 W, which is amplified with a low-noise receiver and compressed using a SAW filter to a pulse that is 60 ns wide. The instrument characteristics and coherent processing techniques result in a range resolution of 4.494 m, assuming a constant index of refraction for ice of n=1.78.

The data are organized into echograms or images where individual radar traces are stacked side-by-side in groups of 1000 (Figure 3). As such, a series of images can be generated for segments of the flight lines, in which layers can be identified. The ranges can be converted into depth and elevation by incorporating surface range and elevation measurements as derived from the Airborne Topographic Mapper (ATM) operating simultaneously on the NASA P-3 aircraft. The ATM elevation retrievals are accurate to better than 10 cm [*Krabill et al.*, 1995].

Data have been acquired along the lines shown in Figure 1. In the present discussion, we focus only on a single flight, May 14, 1999, shown in Figure 2. This flight line not only passes through the GRIP ice core site, where dating of internal layers is possible, but also crosses over itself allowing for a check of consistency at a crossover point and the azimuthal dependence of the measurements.

3. Method

The layer tracing is accomplished primarily through automated means, but it has an interactive component to insure accuracy and retrieve layers where "drop-outs" may occur. The first step in the processing is the enhancement of each echogram to visually optimize the echogram display. Because the radar return strength diminishes with depth due to beam divergence and energy losses in the medium (Figure 3b), the returns from the deeper ice are weaker than those from the shallower regions. We have found that layers can be most clearly seen at all depths when returns below 400 m are normalized by dividing by an exponential (best fit to 1000 traces between 400 and 2000 m depth and set to 1 where returns are below noise level). This visual enhancement

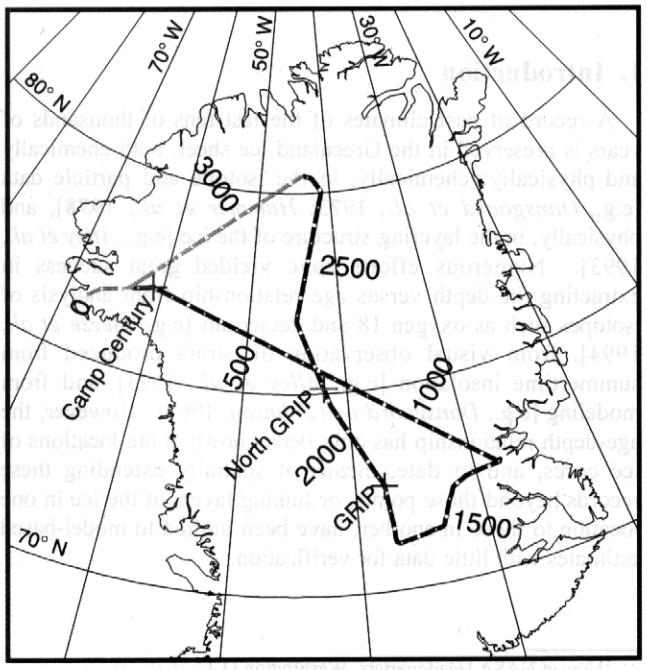

Figure 2. Flight line for May 14, 1999. Layers were traced for both of the black segments (results are shown in Figures 3 and 4). The open circles are spaced 100 km apart along the flight, and the numbers indicate the locations every 500 km along the flight. These along-flight coordinates can be matched to the bottom axis scales in Figures 3a and 4, Plate 1, and Figure 6.

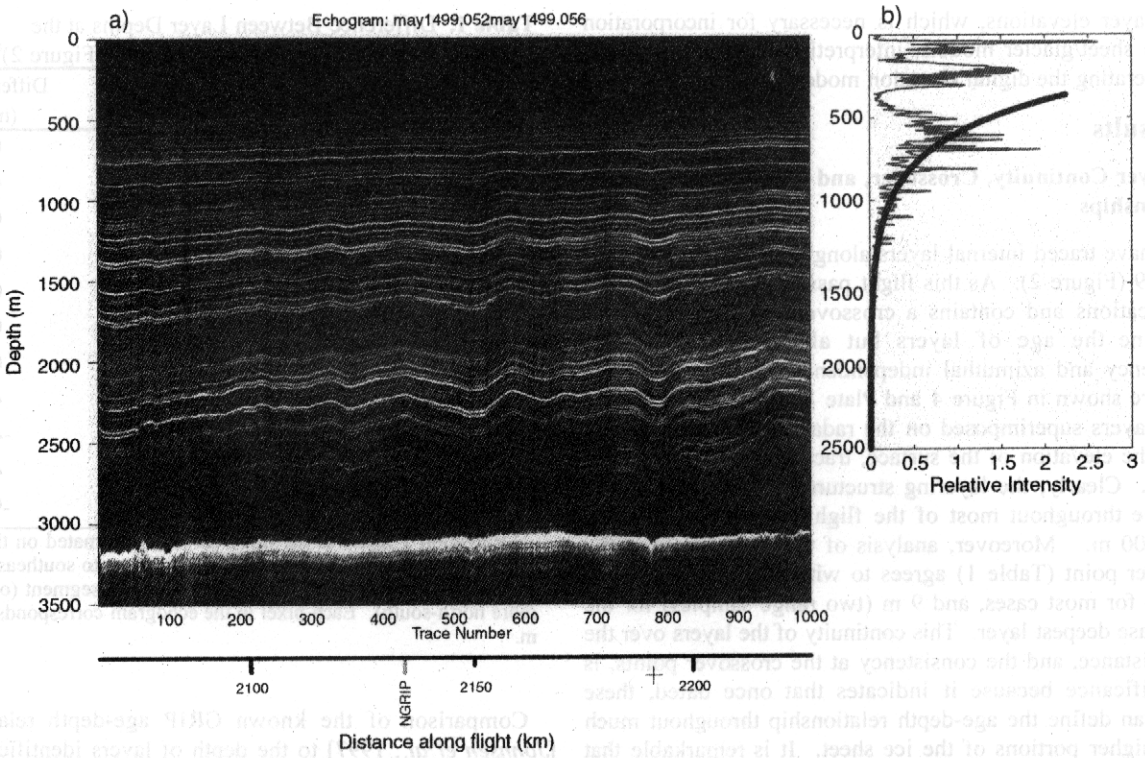

Figure 3. (a) Radio echogram in the vicinity of north GRIP along the northwest ridge of the Greenland ice sheet. (b) Relative intensity of a single trace showing the diminishing radar return with depth and the value of the exponential function applied to each trace in the echogram to visually enhance the deeper layers. The echogram in Figure 3a has this function applied.

assists the operator in identifying layers and verifying results and removes the exponential tail off which would impact the correlations.

The layers can then be traced within and across echograms using a combination of cross-correlation and peak-following techniques, which we have coded into a graphical-interface-driven Matlab routine. The user identifies a reflecting layer within the visually enhanced echogram, which appears as a bright line, then places and clicks the cursor on or near that layer. The software then identifies the strongest return within ±2 pixels, as the layer in that single vertical profile that is to be traced horizontally throughout the echogram. Using a tapered window 40 pixels wide and centered at the local peak, the cross-correlation method extracts a segment of that profile, then searches for that pattern in the next profile along the flight line. When the strongest correlation (i.e., the best pattern match above the background within a limited vertical range) is found, the center of the corresponding window is identified as the location of the layer in that adjacent profile. This method is repeated profile by profile until either the layer is fully traced or until the spatial coherence diminishes to the point where an adequate correlation cannot be found above the background. The latter is generally the case in the percolation zone at lower elevations where the ice is warmer and different backscatter characteristics make distinguishing the layer from its surroundings very difficult.

A peak-following routine is also used to complement the correlation pattern matching. As in the pattern-matching approach, a peak is identified by the user in a single profile, and the software searches adjacent profiles for the strongest return within a five-pixel range around the original depth. Because it is a simpler routine, the peak following is computationally more efficient and effective in areas where the layer pattern may be ambiguous, but a distinct peak is visible. Conversely, in instances where the peak may fade somewhat, but the pattern is preserved, the correlation technique is more appropriate.

After a layer is traced within an echogram, the operator then can visually inspect the automated picks and accept or reject portions of the computer interpretation. When needed, the operator may eliminate sections of the traced layer and pick new starting points by hand, providing the ability to jump fading regions and regions where noise confuses the correlations but where a layer can be seen.

Finally, the software allows a check on the layer picking by warping the radar profile mathematically so that the selected layer and the surface of the ice are both flat. This allows rapid identification of points at which the layer tracing has jumped from one layer to another, as all layers other than the traced one will be offset in the mathematically warped image.

The layer tracing has a subjective aspect to it but only in areas where the fading is pervasive. These areas typically lie below 1500 m elevation and may be related to noise introduced by backscatter from the percolation zone in the surface firn. Much of the high interior has simple records and can be readily traced.

When the layers are traced, they are merged with precise elevation data acquired by the ATM. The ATM elevations are accurate to within 10 cm root-mean-square (RMS) [*Krabill et al.*, 1995]. As the two sets of instruments share the GPS time tag, linking the two is accomplished fairly easily. By combining the data sets, the layer depths can be converted to

actual layer elevations, which is necessary for incorporation into ice sheet/glacier models, interpreting ice flow dynamics and generating the digital elevation models.

4. Results

4.1 Layer Continuity, Crossover, and Age-Depth Relationships

We have traced internal layers along the flight line of May 14, 1999 (Figure 2). As this flight passes through several ice core locations and contains a crossover point, we not only determine the age of layers but also verify their self-consistency and azimuthal independence. Results from the flight are shown in Figure 4 and Plate 1. Figure 4 shows the traced layers superimposed on the radar echograms. Plate 1 shows the elevation of the surface, traced internal layers, and the bed. Clearly, the layering structure is maintained and is traceable throughout most of the flight path in areas higher than 1500 m. Moreover, analysis of the layer height at the crossover point (Table 1) agrees to within 4.5 m (one range sample) for most cases, and 9 m (two range samples) for the worst-case deepest layer. This continuity of the layers over the flight distance, and the consistency at the crossover points, is of significance because it indicates that once dated, these layers can define the age-depth relationship throughout much of the higher portions of the ice sheet. It is remarkable that differences were zero (i.e., below radar resolution) for more than half of the 11 layers. The discrepancy increased slightly with depth but never exceeded two range samples for the layers traced, even at depths of nearly 2.5 km.

Table 1. Difference Between Layer Depths at the Crossover Point of the May 14 Flight Line (Figure 2)[a]

Layer	Elevation 1 (m)	Elevation 2 (m)	Difference (m)
1	597.7	597.7	0.0
2	660.6	656.1	4.5
3	777.5	777.5	0.0
4	1078.6	1078.6	0.0
5	1213.4	1213.4	0.0
6	1447.1	1447.1	0.0
7	1510.0	1510.0	0.0
8	1568.4	1563.9	4.5
9	2013.3	2008.8	4.5
10	2211.1	2206.6	4.5
11	2332.4	2341.4	-9.0

[a] Elevation 1 refers to the layer elevation estimated on the first segment of the flight (oriented more northwest to southeast), and elevation 2 refers to the estimate on the second segment (oriented more north-south). Each pixel in the echogram corresponds to 4.5 m.

Comparison of the known GRIP age-depth relationship [*Johnsen et al.*, 1997] to the depth of layers identified at the GRIP site allows us to estimate the age of each layer. To compare the radar-measured depth to the depth in the ice core, we have added a correction of 8 m to the radar-measured depth to account for higher radar velocity in the firn than the

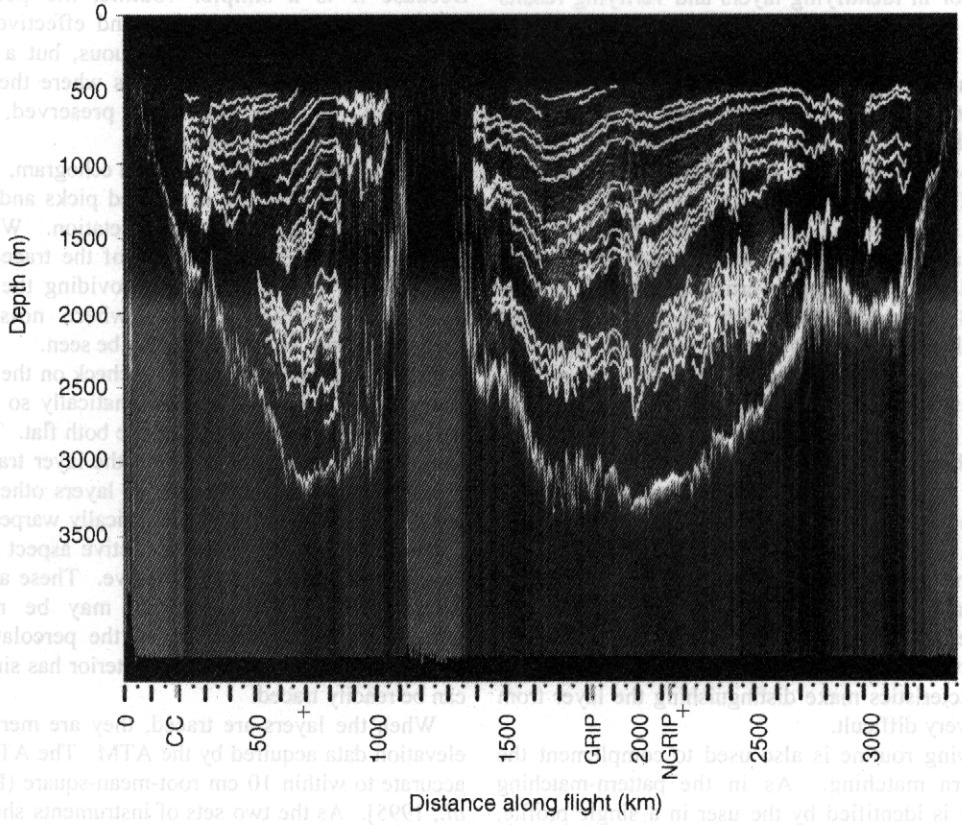

Figure 4. Combined echograms for the entire flight line with traced internal layers overlaid as thick white lines. Lowest reflection is the bed.

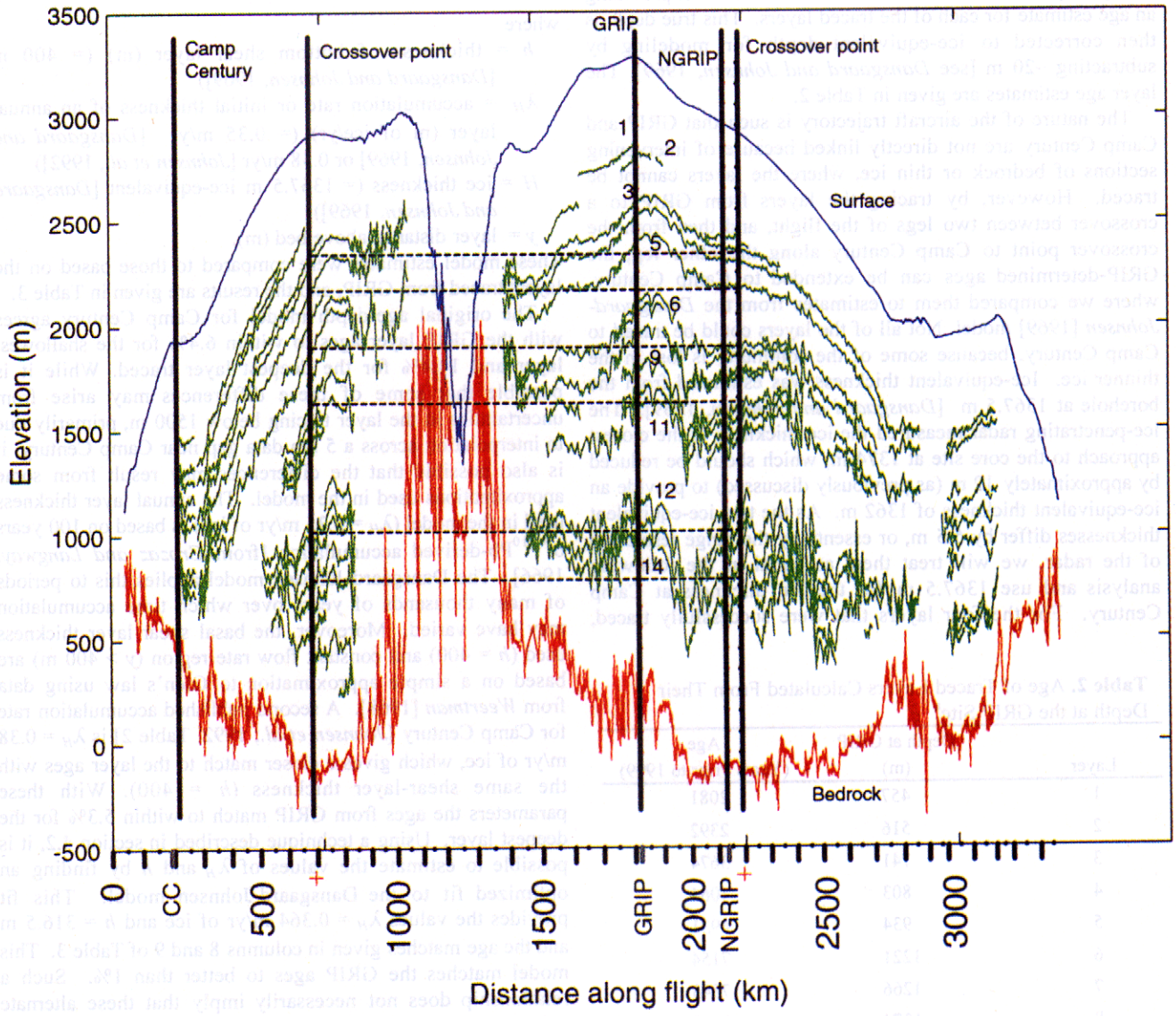

Plate 1. Elevations of traced internal layers and the bed based on their depth below the surface and the surface elevation determined by the ATM laser altimeter [*Krabill et al.*, 1995]. The horizontal lines connecting the crossover points show a sample of the layers discussed in Table 1. The layers at the GRIP site are numbered for reference to Table 2.

constant radar velocity assumed for ice. This correction is found by integrating the reciprocal of the density-dependent velocity [*Kovacs et al.*, 1995] (i.e., the time required to travel a meter) over a depth/density profile for the top 100 m in Greenland [*Paterson*, 1994, Table 2.3, Site A], and using the resulting time interval to determine the distance traveled in solid ice over the same interval. The difference in distance is 8 m, which when added to the radar-determined depth using a constant velocity in ice gives the true depth below the surface [see *Hempel et al.*, 2000]. The true depth can be matched to the age-depth relation determined for the GRIP core, providing an age estimate for each of the traced layers. This true depth is then corrected to ice-equivalent depth for modeling by subtracting ~20 m [see *Dansgaard and Johnsen*, 1969]. The layer age estimates are given in Table 2.

The nature of the aircraft trajectory is such that GRIP and Camp Century are not directly linked because of intervening sections of bedrock or thin ice, where the layers cannot be traced. However, by tracing the layers from GRIP to a crossover between two legs of the flight, and then from the crossover point to Camp Century along the other leg, the GRIP-determined ages can be extended to Camp Century, where we compared them to estimates from the *Dansgaard-Johnsen* [1969] model. Not all of the layers could be traced to Camp Century, because some of the continuity is lost in the thinner ice. Ice-equivalent thickness was estimated from the borehole at 1367.5 m [*Dansgaard and Johnsen*, 1969]. The ice-penetrating radar measured the ice thickness at the closest approach to the core site at 1374 m, which should be reduced by approximately 12 m (as previously discussed) to provide an ice-equivalent thickness of 1362 m. As the two ice-equivalent thicknesses differ by 5.5 m, or essentially the range resolution of the radar, we will treat them as equal in the following analysis and use 1367.5 m for the ice thickness at Camp Century. For the four layers that were successfully traced, layer ages (t) were estimated using the Dansgaard-Johnsen model according to equations (1) and (2) [*Dansgaard and Johnsen*, 1969, equations (12) and (15)]:

$$t = \frac{(2H-h)}{2\lambda_H}\ln\frac{2H-h}{2y-h}, \qquad h \le y \le H, \tag{1}$$

$$t = \frac{(2H-h)}{\lambda_H}\left(\frac{h}{y}-1\right)+t_h, \qquad 0 \le y \le h, \tag{2}$$

where

h = thickness of bottom shear layer (m) (= 400 m [*Dansgaard and Johnsen*, 1969])

λ_H = accumulation rate or initial thickness of an annual layer (m of ice/yr) (= 0.35 m/yr [*Dansgaard and Johnsen*, 1969] or 0.38 m/yr [*Johnsen et al.*, 1992])

H = ice thickness (= 1367.5 m ice-equivalent [*Dansgaard and Johnsen*, 1969])

y = layer distance above bed (m).

These model estimates were compared to those based on the layers traced from GRIP, and the results are given in Table 3.

The original age-depth model for Camp Century agrees with the GRIP layer ages to within 6.4% for the shallowest layer and 14.4% for the deepest layer traced. While it is possible that some of these differences may arise from uncertainties in the layer tracing below 1500 m, primarily due to interpolation across a 5 km data gap near Camp Century, it is also possible that the differences may result from some approximations used in the model. The annual layer thickness used in the model (λ_H = 0.35 m/yr of ice) is based on 100 years of ^{210}Pb-derived accumulation [from *Crozaz and Langway*, 1966]. The Dansgaard-Johnsen model applies this to periods of many thousands of years over which time accumulation may have varied. Moreover, the basal shear layer thickness used (h = 400) and constant flow rate region (y > 400 m) are based on a simple approximation to Glen's law using data from *Weertman* [1968]. A second published accumulation rate for Camp Century [*Johnsen et al.*, 1992, Table 2] is λ_H = 0.38 m/yr of ice, which gives a closer match to the layer ages with the same shear-layer thickness (h = 400). With these parameters the ages from GRIP match to within 5.3% for the deepest layer. Using a technique described in section 4.2, it is possible to estimate the values of λ_H and h by finding an optimized fit to the Dansgaard-Johnsen model. This fit provides the values λ_H = 0.364 m/yr of ice and h = 316.5 m and the age matches given in columns 8 and 9 of Table 3. This model matches the GRIP ages to better than 1%. Such a relationship does not necessarily imply that these alternate values are any more valid than those originally used but does suggest that age differences between the two approaches are reasonable and within the uncertainty of some of the modeling and measurement parameters.

Table 2. Age of Traced Layers Calculated From Their Depth at the GRIP Site[a]

Layer	Depth at GRIP (m)	Age (Years Prior to 1999)
1	457	2081
2	516	2392
3	741	3674
4	803	4064
5	934	4931
6	1221	7154
7	1266	7543
8	1374	8569
9	1531	10274
10	1657	12612
11	1725	14051
12	2170	34375
13	2282	41971
14	2367	48152

[a] Age-depth relationships are from Johnsen et al. [1997], provided in digital form by the National Snow and Ice Data Center in Boulder, Colorado (GRIP timescale ss09). Layer ages are given as years prior to 1999, which is the year of the radar measurement, to facilitate comparison with modeled age-depth relations.

4.2 Long-Term Accumulation Rates

It is possible to estimate the long-term accumulation rate given the age-depth relationship provided by layer tracing from a well-dated ice core site. *Dahl-Jensen et al.* [1997, Figure 2b] made an estimate of this type from GRIP to north GRIP using a radar layer with a GRIP age of 4033 years. Their result compared favorably with surface accumulation data. We provide an example of fitting the age-depth data for

Table 3. Comparison of Age Estimates for Internal Layers at Camp Century, Based on Ages Traced from GRIP, With Ages Estimated With the Dansgaard-Johnsen [1969] Model Using Three Different Sets of Parameters Discussed in the Text[a]

Layer	Ice-Equivalent Depth at Camp Century (m)	Age in Years (From GRIP)	Age in Years (D-J Model λ_H=0.35 m/yr, h=400 m)	Percent Difference	Age in Years (D-J Model λ_H=0.38 m/yr, h=400 m)	Percent Difference	Age in Years (Optimized D-J Model Fit λ_H=0.364 m/yr, h=316.5 m)	Percent Difference
3	818	3674	3911	6.4	3602	-2.0	3651	-0.6
4	867	4064	4397	8.2	4049	-0.4	4082	0.4
5	948	4931	5397	9.5	4971	0.8	4945	0.3
7	1096	7543	8627	14.4	7946	5.3	7535	-0.1

[a] Percent difference is 100 x (model age – GRIP age)/(GRIP age).

five traced layers at a site with a Dansgaard-Johnsen model. From the radio-echograms and layer tracing we know the ice thickness and age and depth for several layers; we need to find the best fit values of the accumulation rate λ_H and thickness of the shearing layer h, assuming their values to be constant at a site.

If $t_m(i)$ is the model-determined age (from equation (1) or equation (2)) of a layer at a height above the bed $y(i)$, and $t(i)$ is the layer age determined by tracing from GRIP, then we minimize the misfit function

$$f(\lambda_H, h) = \sum_{i=1}^{n} \left[\frac{t_m(i) - t(i)}{t(i)} \right]^2 \quad (3)$$

over the n = 5 layers at the site, using an unconstrained nonlinear minimization (Nelder-Mead simplex method [*Lagarias et al.*, 1998]) in two dimensions. For layers above the shearing depth this function is (from equations (1) and (3)):

$$f(\lambda_H, h) = \sum_{i=1}^{n} \left[\frac{\left(\frac{(2H-h)}{2\lambda_H} \ln \frac{2y(i)-h}{2H-h} \right) - t(i)}{t(i)} \right]^2 . \quad (4)$$

The difference in age is normalized by the age of the layer to give appropriate weighting, acknowledging that older layers are less precisely dated.

The value of this misfit function over a range of accumulation rates and shear-layer depths, given the age-depth data at the site, is displayed in Figure 5 using a logarithmic grayscale with the dark shades showing the region where the function has low values. We have chosen the five layers to be in the upper half of the ice, so the minimization is very sensitive to the value of the accumulation rate but not to the thickness of the shearing layer. This analysis has been done for most of the flight line considered in this paper, providing an estimate of the long-term accumulation along the flight line, which is compared with the surface-based accumulation rate used by *Thomas et al.* [this issue] in Figure 6. The match is remarkable, with differences of less than 2 cm/yr over most of the plot. Note that this analysis assumes a uniform thinning rate over the time interval and does not include the complication of diverging flow and gradients in accumulation upstream. These are being addressed by an extended analysis. In spite of this shortcoming, the results track the present-day pattern of accumulation and promise to give us insight into Holocene conditions that should provide a useful constraint for the ice sheet modeling community.

5. Conclusions

Internal layers of the higher regions of the Greenland ice sheet retain their structure over large distances and are traceable. Consistency at a crossover between two legs of a flight indicates an isotropic character to the layering. This suggests that the age-depth relationship, once known at a single location, can be spatially extended over hundreds of kilometers. When extended from GRIP to Camp Century, the age-depth relationships agree with the Dansgaard-Johnsen model to within 15%, although minor changes in model parameters improve this considerably. The physical structure of the layering is such that digital elevation models of each traced layer and, subsequently, each identified age can be developed for the higher regions of the ice sheet.

With some fundamental assumptions about the strain rates in the top half of the ice, rough estimates of the long-term

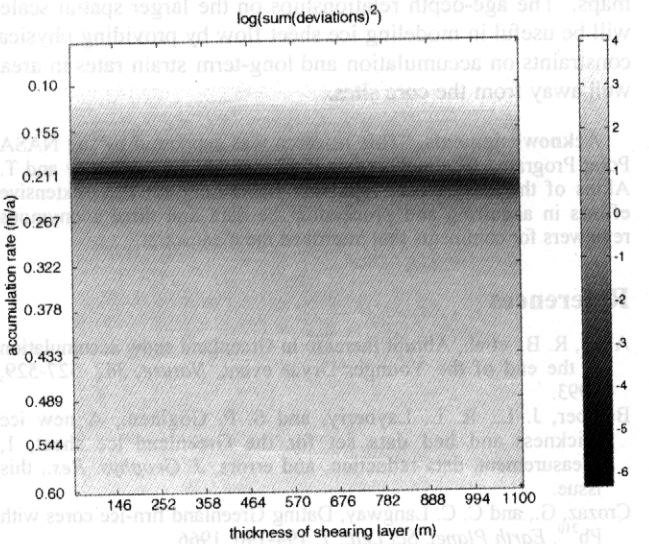

Figure 5. Log 10 value of the minimization (grayscale) plotted as a function of accumulation rate and thickness of basal shearing layer. Note the dark (minimum value) region is narrow for accumulation rate, indicating the minimization is very sensitive to accumulation rate λ_H but not to shear layer thickness h.

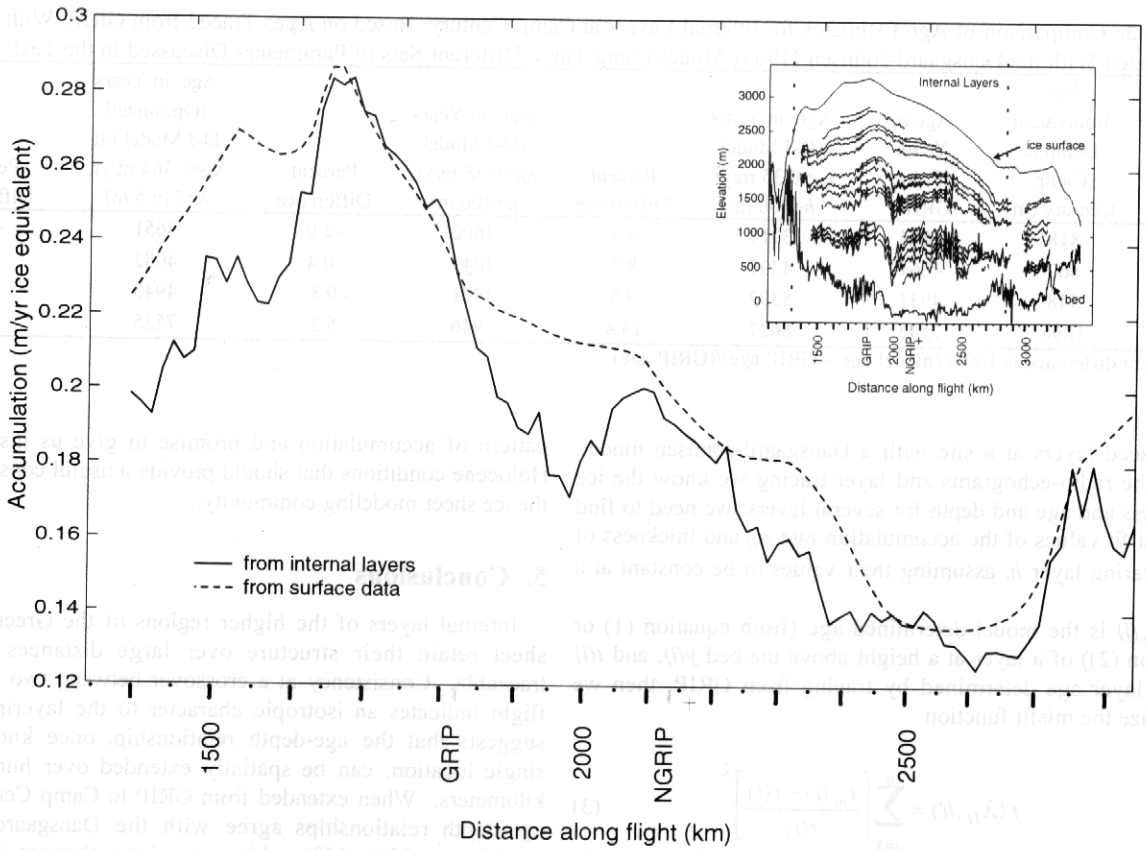

Figure 6. Approximate accumulation estimates from internal layers (solid line) and from surface measurements (dashed line) along a segment of the flight line. The inset shows the layer elevations and the region covered by the estimate (bounded by vertical dashed lines).

accumulation rates have been made that are consistent with present-day accumulation patterns. Once completed for the rest of the ice sheet, more spatially extensive accumulation estimates can be made and compared to present accumulation maps. The age-depth relationships on the larger spatial scales will be useful in modeling ice sheet flow by providing physical constraints on accumulation and long-term strain rates in areas well away from the core sites.

Acknowledgments. This research was supported by the NASA Polar Program. The authors would like to thank J. Legarsky and T. Akins of the NASA Jet Propulsion Laboratory for their extensive efforts in acquiring and processing the data and three anonymous reviewers for comments that improved the manuscript.

References

Alley, R. B., et al., Abrupt increase in Greenland snow accumulation at the end of the Younger Dryas event, *Nature*, *362*, 527-529, 1993.

Bamber, J. L., R. L. Layberry, and S. P. Gogineni, A new ice thickness and bed data set for the Greenland ice sheet, 1, Measurement, data reduction, and errors, *J. Geophys. Res.*, this issue.

Crozaz, G., and C. C. Langway, Dating Greenland firn-ice cores with Pb^{210}, *Earth Planet. Sci Lett.*, *1*, 194-196, 1966.

Dahl-Jensen, D., N. S. Gundestrup, K. Keller, S. J. Johnsen, S. P. Gogineni, C. T. Allen, T. S. Chuah, H. Miller, S. Kipfstuhl, and E. D. Waddington, A search in north Greenland for a new ice-core drill site, *J. Glaciol.*, *43*(144), 300-306, 1997.

Dansgaard, W., and S. J. Johnsen, A flow model and a time scale for the ice core from Camp Century, Greenland, *J. Glaciol.*, *8*(53), 215-223, 1969.

Dansgaard, W., S. J. Johnsen, H. B. Clausen, and N. Gundestrup, Stable isotope glaciology, *Medd. Grøenl.*, *197*(2), 1-53, 1973.

Drewry, D.J. (Ed.), *Antarctica Glaciological and Geophysical Folio*, Scott Polar Res. Inst., Cambrige, England, U.K., 1983.

Gogineni, S., D. Tammana, D. Braaten, C. Leuschen, T. Akins, J. Legarsky, P. Kanagaratnam, J. Stiles, C. Allen, and K. Jezek, Coherent radar ice thickness measurements over the Greenland ice sheet, *J. Geophys. Res.*, this issue.

Gogineni, S., T. Chuah, C. Allen, K. Jezek, and R.K. Moore, An improved coherent radar depth sounder, *J. Glaciol.*, *44*(148), 659-669, 1998.

Gudmundsen, P., Airborne radio echo sounding of the Greenland ice sheet, *Geogr. J.*, *135*, 548-551, 1969.

Gudmundsen, P., Layer echoes in polar ice sheets, *J. Glaciol.*, *15*, 95-101, 1975.

Hammer, C. U., H. B. Clausen, W. Dansgaard, N. Gundestrup, S. J. Johnsen, and N. Reeh, Dating of Greenland ice cores by flow models, isotopes, volcanic debris, and continental dust, *J. Glaciol*, *20*(82), 3-26, 1978.

Hempel, L., F. Thyssen, N. Gundestrup, H. B. Clausen, and H. Miller, A comparison of radio-echo sounding data and electrical conductivity of the GRIP ice core, *J. Glaciol.*, *46*(154), 369-374, 2000.

Jacobel, R. W., and S. M. Hodge, Radar internal layers from the Greenland summit, *Geophys. Res. Lett.*, *22*, 587-590, 1995.

Johnsen, S. J., et al., The $d^{18}O$ record along the Greenland Ice Core Pproject deep ice core and the problem of possible Eemian climatic instability, *J. Geophys Res. 102*, 26,397-26,410, 1997.

Johnsen, S. J., H. B. Clausen, W. Dansgaard, K. Fuhrer, N. Gundestrup, C. U. Hammer, P. Iversen, J. Jouzel, B. Stauffer, and J. P. Steffensen, Irregular Glacial Interstadials Recorded in a New Greenland Ice Core, *Nature*, *359*(6393), 311-313, 1992.

Kovacs, A., A. J. Gow, and R. M. Morey, The in-situ dielectric-constant of polar firn revisited, *Cold Regions Science Technol.*, *23*(3), 245-256, 1995.

Krabill, W. B., R. H. Thomas, C. F. Martin, R. N. Swift, E. B. Frederick, Accuracy of airborne laser altimetry over the Greenland ice sheet, *Int. J. Remote Sens.*, *16*, 1211-1222, 1995.

Lagarias, J. C., J. A. Reeds, M. H. Wright, and P. E. Wright, Convergence properties of the Nelder-Mead simplex method in low dimensions, *Siam J. Optim.*, *9*(1), 112-147, 1998.

Meese, D. A., A. J. Gow, P. Grootes, P. A. Mayewski, M. Ram, M. Stuiver, K. C. Taylor, E. D. Waddington, and G. A. Zeilinski, The accumulation from the GISP2 core as an indicator of climate changes throughout the Holocene, *Science*, *266*(1), 1680-1682, 1994.

Thomas, R., B. Csatho, C. Davis, C. Kim, W. Krabill, S. Manizade, J. McConnell, and J. Sonntag, Mass balance of higher-elevation parts of the Greenland ice sheet, *J. Geophys. Res.*, this issue.

Weertman, J., Comparison between measured and theoretical temperature profiles of Camp Century, Greenland, borehole. *J. Geophys. Res*, *73*, 2691-2700, 1968.

W. Abdalati, Cryospheric Sciences Program, Code YS, NASA Headquarters, 300 E Street NW, Washington, DC, 20546. (wabdalat@hq.nasa.gov)

M. Fahnestock, Earth System Science Interdisciplinary Center, 2207 Computer and Space Sciences Bldg., University of Maryland, College Park, MD 20742. (mark@essic.umd.edu)

S. Gogineni, Radar Systems and Remote Sensing Laboratory, University of Kansas, 2291 Irving Hill Rd., Lawrence, KS 66045. (gogineni@ittc.ukans.edu)

S. Luo, NVI Inc., NASA Goddard Space Flight Center, Code 971, Greenbelt, MD 20771. (sluo@icesat2.gsfc.nasa.gov)

(Received August 15, 2000; revised March 7, 2001; accepted March 19, 2001.)